Singular Value Decomposition of the Time-Frequency Distribution of PPG Signals for Motion Artifact Reduction

Juan F. Rojano and Claudia V. Isaza
SISTEMIC, Facultad de Ingenier á, Universidad de Antioquia UdeA, Calle 70 No. 52-21, Medell ń, Colombia
Email: jfrojanoj@gmail.com, victoria.isaza@udea.edu.co

***Abstract*—Photophethysmography (PPG) is a technique used to measure and record changes in the blood volume of a part of the body and has become an essential tool in the practice of medicine because it is a non-invasive measure of low cost and easy implementation. The PPG signal has been widely used in clinical settings—emergency room, operating room, etc.—but reliable and accurate measurements are achieved only when the patient is at rest. Different indices for assessing the cardiovascular system can be obtained from the analysis of PPG signals. These indices are derived from the analysis of the shape of the PPG signals of patients at rest. When the patient moves, the shape and the spectrum of the PPG signal are altered. This paper presents a new method for the estimation of the main frequency component of PPG signals corrupted with motion artifacts. In addition, the analysis of the singular values obtained with this method allows to estimate the level of noise affecting the PPG signal. The periodicities of the noisy PPG signal can be estimated, simply by reconstructing the signal with its main frequency component and then, detect its zero crossings. The proposed method has a low computational cost. This article compares the performance of the method Singular Value Decomposition of the Time–Frequency Distribution (SVDTFD) with Discrete Wavelet Transform (DWT) and Ensemble Empirical Mode Decomposition (EEMD) by estimating the heart rate from PPG signals with motion artifacts produced by the continuous movement of patients.**

***Index Terms*—photoplethysmography, motion artifacts, singular value decomposition, short–time Fourier transform, discrete wavelet transform, ensemble empirical mode decomposition**

I. Introduction

The photoelectric phethysmography, also known as photoplethysmography, is based on changes in the absorption properties of the tissue and the blood when illuminated by light. The interaction of the different body systems involved in the generation of the PPG signal is an active area of research and debate.

The principle of the technique is simple. The light irradiated from a source (LED) is scattered, reflected and partly absorbed by the tissue and the blood. Part of the scattered radiation go through the skin and is detected by a photodetector. The radiation ranging between red and infrared is the most used because it penetrates several millimeters below the surface of the skin and reaches the blood vessels located in the dermis. This radiation is partially modulated by the periodic changes in the volume of arterial blood, as these cause the corresponding dynamic changes in the absorption of the tissue being irradiated [1]. These variations of the PPG are attributed to the interaction of the arterial and venous blood with cardiac, respiratory and autonomous systems. The general consensus in the medical field is that blood pressure waves propagate along the arteries of the skin, locally increasing and decreasing the volume of blood in the tissues with the same frequency of the heartbeat. Dynamic changes in blood volume depends basically on the characteristics of cardiac function, the size and elasticity of the blood vessels and specific neuronal processes [2]. The intensity of the modulated light that reaches the photodetector generates variations in its output current and is assumed that these changes are related to changes in the arterial blood volume.

The size and technology of this sensor makes it suitable for non-invasive mobile monitoring applications of patients. One of the major disadvantages presented by the use of photoplethysmography on mobile devices, is that PPG signals are highly susceptible to the motion of the patients. The motion artifacts are usually induced by the movement between the sensor and the skin [3]-[5]. This noise considerably reduces the performance of pulse oximeters in its various applications. The motion artifact reduction is not obvious because the components of the PPG signal and the components of the acceleration overlaps and also because the PPG signal is quasi-periodic and non-stationary, making it necessary to use advanced signal processing techniques. Motion artifact reduction is an open research problem. As far as the authors know, the proposed techniques so far are not sufficiently robust to completely reconstruct the PPG signal while the patient is moving.

The Singular Value Decomposition (SVD), Empirical Mode Decomposition (EMD), Discrete Wavelet Transform (DWT) and adaptive filtering methods have shown a very good performance in the reduction of motion artifacts. The SVD as has been proposed [6] has a low performance when the fundamental frequency of the PPG signal changes, and the decomposition obtained

Manuscript received September 18, 2015; revised May 9, 2016.

doi: 10.18178/ijsps.4.6.475-482

depends on the level of distortion generated by the motion artifact. Adaptive Noise Cancellation (ANC) estimates the noise signal from information correlated with the movement of the sensor. This data is highly correlated with the motion artifacts, but is obtained from accelerometers located near the sensor [7], which is beyond the scope of this study. EEMD based methods estimates an approximation of the main frequency component of PPG signals with motion artifacts, but the performance of this decomposition directly depends on the number of ensembles used, which in turn increases the execution time of this algorithm. The DWT estimates the main frequency component of PPG signals with motion artifacts by thresholding the wavelet coefficients [8]. The performance of the proposed method is compared with DWT and EEMD by estimating the heart rate of patients during physical exercise.

This article is organized as follows: Section II presents the SVDTFD, DWT and EEMD methods. Section III presents the case study. Section IV presents the comparison of the SVDTFD, DWT and EEMD methods. Finally, conclusions and future work are presented.

II. Methods

A. Singular Value Decomposition of the Time-Frequency Distribution

The proposed method finds the Singular Value Decomposition (SVD) of the time-frequency distribution obtained with the Short-Time Fourier Transform (STFT). The singular value decomposition identifies and order the dimensions in which the data presents the highest variation and then finds the best approximation of the original data using few dimensions. The application of the SVD to the complex matrix given by the STFT decomposes the time-frequency distribution of the PPG signal in its higher variation components.

1) Singular value decomposition

Let $\boldsymbol{A}$ be a real or complex valued matrix of size $m \times n$ with $m \geq n$. The SVD of $\boldsymbol{A}$ is a factorization of the form.

$$\boldsymbol{A} = \boldsymbol{U}\boldsymbol{\Sigma}\boldsymbol{V}^{\mathsf{T}} \tag{1}$$

where $\boldsymbol{U}^{\mathsf{T}}\boldsymbol{U} = \boldsymbol{V}^{\mathsf{T}}\boldsymbol{V} = \boldsymbol{I_n}$ and $\boldsymbol{\Sigma} = diag(\sigma_1, \dots, \sigma_2)$.

The matrix $\boldsymbol{U}$ of size $m \times m$ consist of m orthonormal eigenvectors associated with the m eigenvalues of $\boldsymbol{A}\boldsymbol{A}^{\mathsf{T}}$ and the matrix $\boldsymbol{V}$ os size $n \times n$ consist of n orthonormal eigenvectors associated with the n eigenvalues of $\boldsymbol{A}^{\mathsf{T}}\boldsymbol{A}$. The columns of $\boldsymbol{U}$ are called *left singular vectors* of $\boldsymbol{A}$ while the columns of $\boldsymbol{V}$ are called *right singular vectors* of $\mathbf{A}$. The columns of $\boldsymbol{U} = [\boldsymbol{u}_1, \dots, \boldsymbol{u}_m]$ corresponding to non-zero diagonal elements of $\boldsymbol{\Sigma}$ span the range of $\mathbf{A}$. The columns of $\boldsymbol{V} = [\boldsymbol{v}_1, \dots, \boldsymbol{v}_n]$ corresponding to zero diagonal elements of $\boldsymbol{\Sigma}$ are a orthonormal basis of the null space of $\mathbf{A}$. The elements σ_i of the diagonal of $\boldsymbol{\Sigma}$ are the non–negative square roots of the eigenvalues of $\boldsymbol{A}^{\mathsf{T}}\boldsymbol{A}$ and are called *singular values*. It holds that $\sigma_1 \geq \cdots \geq \sigma_n \geq 0$. If $rank(\boldsymbol{A}) = r$ then $\sigma_{r+1} = \cdots = \sigma_n = 0$ [9].

The major advantages of the singular value decomposition are: i) The SVD transforms correlated variables into a set of uncorrelated variables that exposes the different relations between the original data. ii) The SVD allows to identify and order the dimensions in which the data show the greatest variation. iii) Finally, once you have identified where the most variation occurs, it is possible to find the best approximation of the original data using a few dimensions (the ones with most variation).

2) Short-Time Fourier transform

The Short-Time Fourier Transform (STFT) represents signals in the form of time–frequency maps of energy—spectrograms. It is used to determine the frequency and phase content of a local section of a signal as it changes over time [10].

The Fourier transform FFT of a continuous real variable signal x is defined as:

$$FFT(f) = \int_{-\infty}^{\infty} x(t) exp^{-j2\pi ft} dt \tag{2}$$

where t is time, f frequency and j is the imaginary unit.

This definition leads to the inversion formula of the Fourier transform:

$$x(t) = \int_{-\infty}^{\infty} FFT(f) exp^{j2\pi ft} df \tag{3}$$

The STFT of a signal $x(t)$ is defined using a window $g(t)$, as:

$$STFT_x^g(t,f) = \int_{-\infty}^{\infty} x(t') g^*(t'-t) exp^{-j2\pi ft'} dt' \tag{4}$$

The spectrogram can be associated with the energy density of x at time t and frequency f, and is defined as:

$$spectrogram\{x(t)\}(t,f) = \left|STFT_x^g(t,f)\right|^2 \tag{5}$$

The inversion formula of the STFT is:

$$x(t') = \iint_{-\infty}^{\infty} STFT_x^g(t,f) g(t'-t) exp^{j2\pi ft'} df dt \tag{6}$$

For a discrete signal $x[k]$, $k \in \mathbb{Z}$ with an analysis window $g[k]$ of length L, the STFT becomes:

$$STFT_x^g[k,l] = \sum_{k'} x[k'] g^*[k'-k] exp^{-j2\pi lk'/L} \tag{7}$$

where $k \in \mathbb{Z}$ and $l = 0, \dots, L-1$.

It is considered the case of a finite signal with N samples $x[k]$, $k = 0, \dots, N-1$. In this case the STFT is a complex value matrix of size $N \times L$ containing information about the phase and the frequency of the signal $x[k]$.

The simplified inversion formula for a discrete signal is:

$$x[k'] = \frac{1}{L\, g^*[0]} \sum_{l=0}^{L-1} STFT_x^g[k',l] exp^{j2\pi lk'/L} \tag{8}$$

The proposed method (Singular Value Decomposition of the Time–Frequency Distribution [SVDTFD]) consist of five stages: *i*) PPG signal filtering in the range $0.5Hz$ to $5Hz$. *ii*) Get the complex value matrix $\boldsymbol{STFT}$ of the PPG signal, where the PPG signal is the discrete signal $x[k]$ in (7). *iii*) Decompose the matrix $\boldsymbol{STFT}$ in its singular values (section *II.A.1*). *iv*) Reconstruct the matrix $\boldsymbol{STFT}$ as:

$$\overline{\boldsymbol{STFT}} = \sum_{i=1}^{N} \boldsymbol{u}_i \sigma_i \boldsymbol{v}_i^{\mathsf{T}} \tag{9}$$

where $\overline{\boldsymbol{STFT}}$ is the reconstructed spectrum, $\boldsymbol{u}_i \sigma_i \boldsymbol{v}_i^{\mathsf{T}}$ is the *i*-th SVDTFD component and n indicates the number of

SVDTFD components to be taken in the reconstruction of the PPG signal. n will be called the *reconstruction level*. *v*) Get the filtered PPG signal by taking the inverse STFT (8) of the matrix $\overline{\boldsymbol{STFT}}$.

B. Discrete Wavelet Transform (DWT)

The Continuous Wavelet Transform (CWT) decompose a continuous signal $x(t)$ into a basis of translated and dilated functions called wavelets:

$$\psi_{a,b} = \frac{1}{\sqrt{a}}\psi\left(\frac{t-b}{a}\right) \tag{10}$$

Provided that the signal $x(t)$ and the mother wavelet $\psi(t)$ are finite energy signals, the CWT is defined as:

$$CWT(a,b) = \frac{1}{\sqrt{a}}\int_{-\infty}^{\infty} x(t)\psi\left(\frac{t-b}{a}\right)dt \tag{11}$$

where a is the scale factor which controls the width (or effective support) of the function ψ and b is the translation factor which controls the temporal localization of the function ψ.

The wavelet coefficients represent the correlation between the wavelet and a localized section of the signal, and they are proportional to the inner product between the signal and the different wavelets $\psi_{a,b}$.

If the wavelets are generated only by integer translations and dilatations of the mother wavelet $\psi(t)$, it is generated a family of functions of the form:

$$\psi_{j,k}(t) = 2^{j/2}\psi(2^j - k) \quad j,k \in \mathbb{Z} \tag{12}$$

where the factor $2^{j/2}$ holds a constant norm independent of the scale j. This family of functions is called the *wavelet expansion set*. The mother wavelet $\psi(t)$ has an associated scale function $\phi(t)$ and both form an orthonormal basis for the expansion of one-dimensional signals. Both functions allows to approximate a finite energy signal $x(t)$ as [11].

$$x(t) = \sum_k c_{j_0,k}\phi_{j_0,k}(t) + \sum_k\sum_j d_{j,k}\psi_{j,k}(t) \tag{13}$$

where $j,k \in \mathbb{Z}^+$, $c_{j_0,k}$ are the scale coefficients, j_0 is the space of lower resolution, and $d_{j,k}$ are the wavelet coefficients.

The Discrete Wavelet Transform (DWT) decomposes the signal using filter banks. The filter banks consist of pairs of quadrature mirror filters, one a Low Pass Filter (LPF) and the other a High Pass Filter (HPF). This filter banks decompose the signal in different scales (Fig. 1).

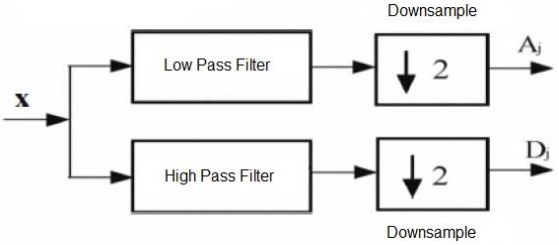

Figure 1. DWT filter banks [8].

The A_j are the approximated coefficients, and they are the output of the LPF. The D_j are the detailed coefficients, and they are the output of the HPF [8].

1) DWT for motion artifact reduction

Provided that the noisy signal $x(t)$ is sparse in the wavelet domain, which is usually the case, the DWT is expected to distribute the total energy of the noiseless signal in only a few wavelet components with high amplitude. As a result, the amplitude of most of the wavelet components is attributed to noise only. The general procedure to reduce the noise of a signal is to zeroing all the detailed coefficients that are smaller than a threshold T that is related to the noise level [12]. The most important thresholdind operators are hard thresholding:

$$\rho(c) = \begin{cases} c, & if\ |c| > T \\ 0, & if\ |c| \le T \end{cases} \tag{14}$$

and soft thresholding:

$$\rho(c) = \begin{cases} sgn(c)(|c| - T), & if\ |c| > T \\ 0, & if\ |c| \le T \end{cases} \tag{15}$$

where c is each wavelet coefficient and T is the chosen threshold.

C. Hilbert-Huang Transform (HHT)

1) Empirical Mode Decomposition (EMD)

The Empirical Mode Decomposition (EMD) [13] is an adaptive method that allows to analyze signals which can be non-stationary or from non-linear systems. It decomposes the signal directly in the time domain — totally dependent on data—in oscillations of different frequencies. At the end of the decomposition, the original signal can be expressed as a sum of amplitude and frequency modulated signals called Intrinsic Mode Functions (IMF) plus a trend that can be monotonic or constant:

$$x(t) = \sum_{j=1}^{n} h_j(t) + r_n(t) \tag{16}$$

where $x(t)$ is the noisy signal, n is the number of IMFs, $h_j(t)$ is the j-th IMF and $r_n(t)$ is the trend of $x(t)$. For a signal to be considered an IMF must satisfy two conditions *i*) The number of extrema and the number of zero crossings must be equal or differ at most by one. *ii*) At any time instant, the mean value of the upper and lower envelopes is zero.

The second condition implies that an IMF is stationary, but can have amplitude modulations and changes in its instantaneous frequency.

The algorithm 1 describes the principle of EMD [14].

Algorithm 1 EMD algorithm

1: $r_0(t) = x(t), j = 1$
2: **while** $1 = 1$ **do**
3: $h_0(t) = r_{j-1}(t), k = 1$
4: **while** *stopping criteria* **do**
5: Locate local maxima and minima of $h_{k-1}(t)$
6: Cubic spline interpolation to define upper and lower envelop of $h_{k-1}(t)$
7: Calculate mean $m_{k-1}(t)$ from upper and lower envelop of $h_{k-1}(t)$
8: $h_k(t) = h_{k-1}(t) - m_{k-1}(t)$
9: $k = k + 1$
10: **end while**
11: $h_j(t) = h_k(t)$

12: $r_j(t) = r_{j-1}(t) - h_j(t)$
13: $j = j + 1$
14: **if** $r_j(t)$ has only one extrema **then**
15: **break**
16: **end if**
17: **end while**
18: $r_n(t) = r_j(t)$

Usually the *stopping criteria* is when the number of extrema and zero crossings are equal or differ at least in one, and that difference remains constant for several consecutive steps of the algorithm

In some cases EMD may experience the *mode mixing*, which is presented as oscillations of very disparate amplitude in a mode, or the presence of very similar oscillations in different modes. To overcome this problem, it was proposed the Ensemble Empirical Mode Decomposition (EEMD) [15], [16]. EEMD defines the *true* IMF components (denoted as $\overline{IMF}$) as the mean of the corresponding IMFs obtained via EMD over an ensemble of trials, generated by adding different realizations of white noise of finite variance to the original signal $x(t)$. The algorithm 2 describes the principle of EEMD [16].

Algorithm 2 EEMD algorithm

1: Generate $x^i(t) = x(t) + \beta\omega^i(t)$, where $\omega^i(t), i = 1, \dots, I$ are different realizations of zero mean unit variance Gaussian noise.
2: Fully decompose by EMD (Alg 1) each $x^i(t), i = 1, \dots, I$ getting their modes IMF_j^i, where $j = 1, \dots, J$ indicates the modes of $x^i(t)$
3: $\overline{IMF}_j(t) = \frac{1}{I}\sum_{i=1}^{I} IMF_j^i(t)$, where $\overline{IMF}_j(t)$ is the *j*-th mode of $x(t)$

2) Hilbert spectral analysis

The instantaneous frequency and the local energy for each IMF can be derived using the Hilbert transform.

The Hilbert transform $y(t)$ of a function $x(t)$ of L^p class is:

$$y(t) = \frac{1}{\pi} P \int_{-\infty}^{\infty} \frac{x(t)}{t-\tau} dt \tag{17}$$

where *P* is the Cauchy principal value of the singular integral. From the function $x(t)$ and its Hilbert transform $y(t)$ it is obtained the analytic function.

$$z(t) = x(t) + jy(t) = a(t)exp^{i\theta(t)} \tag{18}$$

where *j* is the imaginary unit:

$$a(t)(x^2 + y^2)^{1/2}, \theta(t) = \tan^{-1}\frac{y}{x} \tag{19}$$

where the function $a(t)$ is the instantaneous amplitude and the function $\theta(t)$ is the instantaneous phase. The instantaneous frequency is:

$$IF = \frac{1}{2\pi}\frac{d\theta(t)}{dt} \tag{20}$$

and the local energy is:

$$E(t) = \frac{1}{2}a(t)^2 \tag{21}$$

3) HHT for motion artifact reduction

The conventional EMD denoising technique identifies each IMF to be noise-only case or noise-signal case by energy level and partially reconstructs the signal using only the information dominant IMFs. Nevertheless the motion artifacts scatter on every scale so that the conventional approach is not capable of reducing the motion artifacts effectively [17].

A more effective denoising procedure is based on thresholding each IMF [12], [17]. The threshold operator used is soft. the *i*-th IMF is sliced into the segments $h^i(Z_j^i)$ where the Z_j^i represent the time interval between the *j*-th and the $j+1$-th zero crossing $[z_j^i, z_{j+1}^i]$. The parameter used for the soft thresholding are the energy level $E_i(t)$ of each IMF and the range of instantaneous frequency $IF_i(t)$. The *j*-th thresholded segment $\tilde{h}^i$ of the *i*-th IMF is:

If $|h^i(r_j^i)| > T_i$ and $0.5 \leq IF_i(Z_j^i) \leq 10$ then:

$$\tilde{h}^i(Z_j^i) = h^i(Z_j^i)\frac{|h^i(r_j^i)| - T_i}{|h^i(r_j^i)|} \tag{22}$$

in any other case $\tilde{h}^i(Z_j^i) = 0$, where $h^i(r_j^i)$ is the amplitude of the extremum of each time interval Z_j^i and:

$$T_i = \sqrt{E_i} \times \tau_{thr}, \tag{23}$$

III. Case Study

This section discusses the different levels of reconstruction obtained with the SVDTFD method applied to PPG signals of patients at rest and in continuous movement. This is done by varying the number of SVDTFD components n used in the spectrum reconstruction of the PPG signal (9). The signals of patients at rest and walking correspond to the testing phase of the project "Sistema de Vigilancia de Eventos de Pacientes Ambulatorios en Riesgo Cardiovascular" developed in the center of excellence ARTICA in cooperation with the faculties of medicine and engineering of the Universidad de Antioquia. The signals of patients during physical exercise were obtained of TROIKA [18].

A. Singular Value Decomposition of the Time-Frequency Distribution

The parameters of this method are the same as those of STFT: i) Analysis window. ii) Length of the window. iii) Overlapping.

1) Analysis of PPG signals without motion artifacts

For a noiseless PPG signal, the SVDTFD obtains the main frequency component of the signal and its harmonics. Fig. 2 shows the singular value for each SVDTFD component of the matrix ***STFT*** of a healthy patient at rest.

As can be seen from Fig. 2, the first 6 SVDTFD components account for 93% of the total variance of the PPG signal. The first SVDTFD component account for 50% of the total variance of the signal, and it is equivalent to the heart rate of the patient. Fig. 3 shows the reconstructed signal (solid line) by varying the number of

SVDTFD components n in (9). The dotted-dashed line represents the original PPG signal.

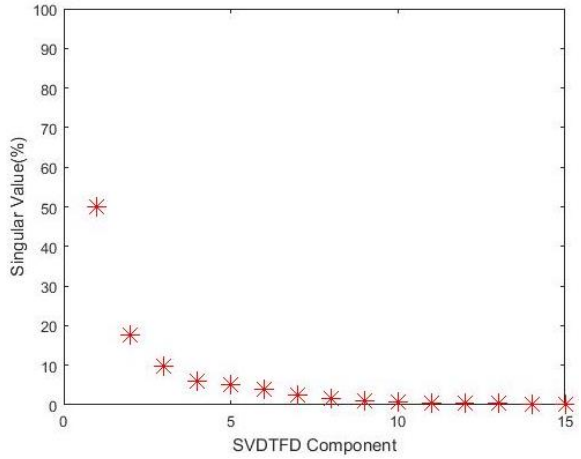

Figure 2. Singular values of a noiseless PPG signal.

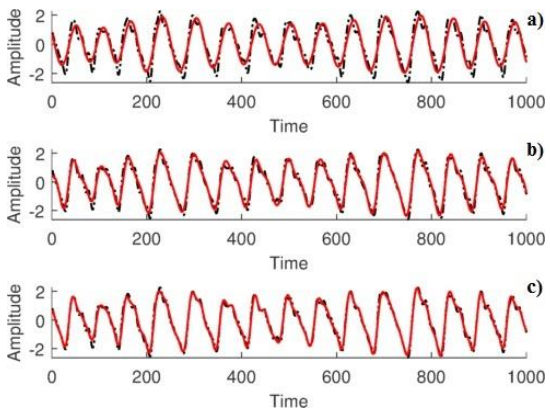

Figure 3. Different reconstruction levels of a noiseless PPG signal with the SVDTFD. a) First SVDTFD component $n = 1$.b) 1 and 2 SVDTFD components $n = 2$. c) 1 to 3 SVDTFD components $n = 3$.

As can be seen from Fig. 3, the first SVDTFD component $i = 1$ corresponds to the main frequency component of the PPG signal (heart rate). Each of the following SVDTFD components ($i \geq 2$) correspond to a harmonic of the PPG signal. The first 4 SVDTFD components account for 85% of the variance of the PPG signal, which is enough to analyze the PPG signal. Since all PPG signals are different, is proposed to reconstruct any noiseless PPG signal with the first $n = 4$ SVDTFD components, which account for at least the 80% of the total variance of the signal.

With noiseless PPG signals, this method acts as a filter that retrieves the main components of the PPG signal. Remember that PPG signals are quasi-periodic and non-stationary, which makes that the frequency components and the phase of the signal changes over time. SVDTFD is able to take into account those changes and adapt to them. It follows that the reconstructed PPG signal for each level of reconstruction is in phase with the original PPG signal (Fig. 3).

2) Analysis of PPG signals with motion artifacts

When the PPG signal is corrupted with motion artifacts, this method establishes the noise level contaminating the signal and finds its main frequency component. The following analysis want to show the variation of the singular values of each SVDTFD component according to the noise level contaminating the PPG signal. Fig. 4 shows the singular value of each SVDTFD component of the matrix ***STFT*** of a healthy patient in continuous motion (walking at normal pace).

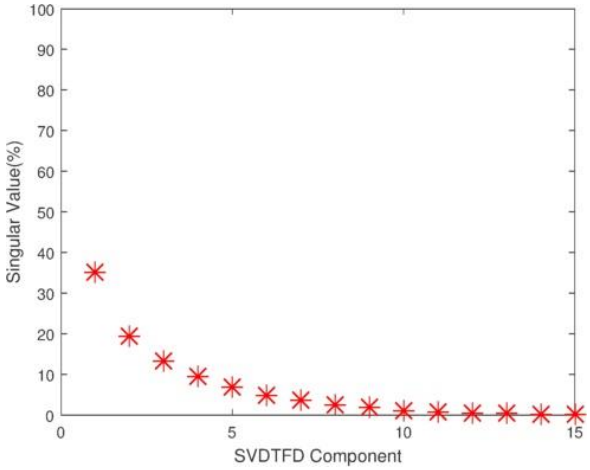

Figure 4. Singular values of a PPG signal with moderate motion artifacts.

In Fig. 4 can be noticed that the variance contributed by the first 7 SVDTFD components is 93%. The variance accounted for the first SVDTFD component is 35.5%. When moderate motion artifact occurs in the PPG signal, the variance of the first component is reduced compared to the same signal in a range without motion artifacts, while the variance of the SVDTFD components from 2 to 4 increases. Remember that the nature of the motion artifacts is random, therefore its power contribution at each frequency is also random. Through the analysis of signals of walking patients it is concluded that the power contribution of moderate motion artifacts at each frequency are higher for the frequency components 2 and 3 of the PPG signal. The foregoing agrees with that the movements with acceleration between 0.7Hz and 2.5Hz affect the PPG signal [7]. Fig. 5 shows a segment of the signal under study and its first reconstruction level $n = 1$. The solid line represents the reconstructed signal and the dotted-dashed line represents the original PPG signal.

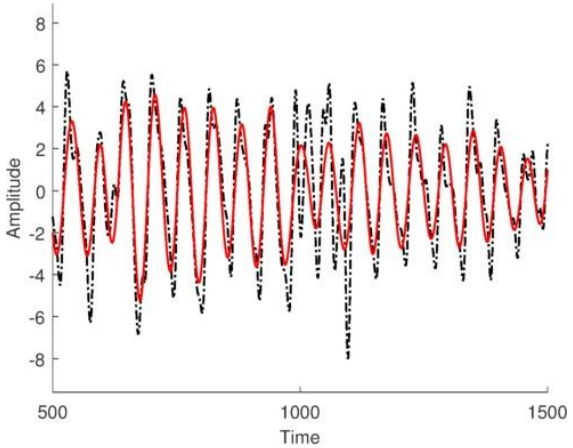

Figure 5. First reconstruction level of the PPG signal of a healthy patient in moderate continuous movement.

Fig. 6 shows the singular values for a signal corrupted with intense motion artifacts (patient during physical exercise), the variance contributed by the first 13 SVDTFD components is 93%. The variance accounted for the first SVDTFD component is 28%.

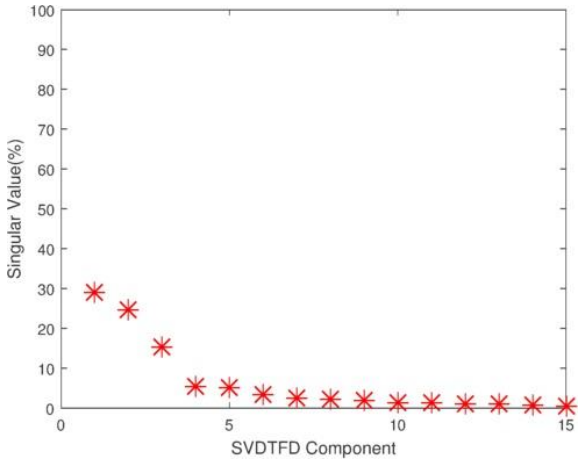

Figure 6. Singular values of a PPG signal with intense motion artifacts.

Fig. 7 shows a segment of the signal under study and its first reconstruction level $n = 1$.

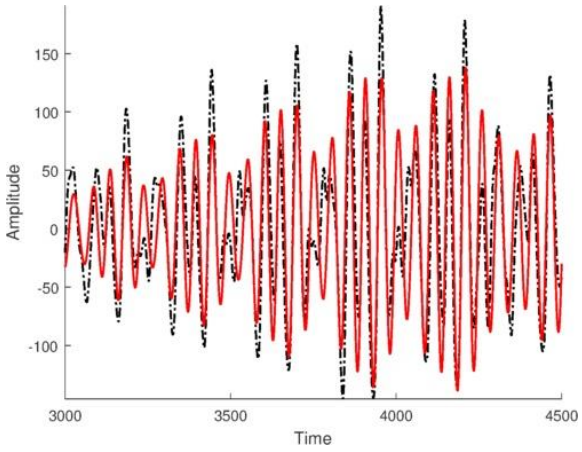

Figure 7. First reconstruction level of the PPG signal of a healthy patient during physical exercise.

As the movement of the patient increases, the variance of the principal components of the PPG signal decreases and the variance of the others components increases. This behavior occurs because as the patient movement increases, the power and the frequency range of motion artifacts also increase.

B. Discrete Wavelet Transform

The parameters of DWT are: i) The Threshold selection rule $TPTR$. ii) The thresholding operator (soft or hard). iii) The Wavelet decomposition level N. *iv*) The Mother wavelet. The parameters used are: i) Universal threshold. ii) Soft thresholding operator. iii) $N = 4$. *iv*) Daubechies 44 [19]. This parameters were selected from the analysis of the signals in Section III.A. Thresholding wavelet coefficients allows to find the main frequency component of PPG signals, but the reconstructed signal is out of phase with the original.

C. Hilbert-Huang Transform

The parameters of EEMD are: i) The amplitude of the added white noise β. ii) The number of ensembles I. iii) The value of the multiply parameter τ_{thr}. The parameters used are: i) β=0.28 . ii) I=30 . iii) τ_{thr}=0.18 . This parameters were selected from the analysis of the signals in Section III.A. IMF thresholding allows to find the main frequency component of PPG signals, but the reconstructed signal is out of phase with the original. A higher number of ensembles improves the filtering, but the execution time becomes prohibitive.

IV. Comparison of the Methods SVDTFD, DWT, EEMD for the Estimation of the Heart Rate during Physical Exercise

The comparison of the SVDTFD, DWT and EEMD methods for the reduction of motion artifacts consist in estimating the heart rate (bpm) from the PPG signal of a patient during physical exercise. The analysis was made from PPG signals of 11 people in continuous movement. During data recording, each subject ran on a treadmill with changing speeds. The running speeds changed as follows: at rest for 30s, at 6km/h for one minute, at 12km/h for one minute, at 6km/h for one minute, at $12km/h$ for one minute, at rest for 30s. The sensor used was a bracelet. The heart rate values are calculated in windows of $8s$ length. Two successive windows overlap by 6s . The signals used for the comparison of the methods were obtained from TROIKA [18].

The performance measures normally used for this type of estimates are:

- The Average Absolute Error (AAE) measured in bpm and is defined as:

$$AAE = \frac{1}{N}\sum_{i=1}^{N}|BPM_{est}(i) - BPM_{true}(i)| \qquad (24)$$

where N is the number of estimates.

- The Average Absolute Percentage Error (AAEP) is defined as:

$$AAEP = \frac{1}{N}\sum_{i=1}^{N}\frac{|BPM_{est}(i) - BPM_{true}(i)|}{BPM_{true}(i)} \qquad (25)$$

Table I shows the average absolute error for each signal and each method. Table II shows the average absolute percentage error for each signal and each method

TABLE I. Average Absolute Error in the Estimation of the Heart Rate

Patient	SVDTFD(bpm)	DWT(bpm)	EEMD(bpm)
1	24.03	21.92	19.68
2	21.64	16.89	23.16
3	7.26	10.70	13.78
4	1.03	1.74	17.36
5	5.75	10.45	6.89
6	0.57	2.61	6.92
7	3.61	8.32	12.63
8	2.02	5.00	6.07
9	19.87	18.13	62.82
10	5.10	4.96	41.17
11	15.57	16.05	25.52
Mean±std	8.87±8.88	9.73±7.19	19.67±17.47

As can be seen from Table I and Table II, the SVDTFD method has the highest performance and the EEMD method has the lowest performance. In some cases the error in the estimate exceeds the 15%, because for certain movements the motion artifacts obscures the heart rate information of the PPG signal.

TABLE II. AVERAGE ABSOLUTE PERCENTAGE ERROR IN THE ESTIMATION OF THE HEART RATE

Patient	SVDTFD(%)	DWT(%)	EEMD(%)
1	20.33	19.42	16.04
2	16.83	13.70	16.48
3	6.35	9.63	10.00
4	0.76	1.33	11.09
5	5.11	9.42	5.71
6	0.44	2.25	4,82
7	3.34	6.92	9.63
8	2.12	5.06	4.97
9	11.94	10.81	38.18
10	3.55	3.45	25.29
11	11.54	11.95	16.65
Mean±std	6.86±6.76	7.83±5.74	13.24±10.43

V. CONCLUSIONS

This paper presented a simple method to find the main frequency components of PPG signals by means of the singular value decomposition of the time-frequency distribution given by the STFT. When the PPG signal is corrupted with motion artifacts, the first SVDTFD component corresponds with the main frequency component of the PPG signal (heart rate).

The application of the method was presented for signals of healthy patients at rest, walking and during physical exercise. It is concluded that the singular values given by the proposed method allow to analyze the state of motion of the patient. The time variation of the singular values are correlated with the changes in the frequency components of the PPG signal generated by motion artifacts.

A comparison was made with the DWT and EEMD methods, using them to estimate the heart rate from PPG signals registered during physical exercise of the patient.

When comparing the SVDTFD with the other two methods, it was found that the SVDTFD has the benefit of finding the main frequency component of PPG signals corrupted with motion artifacts by only reconstructing the signal with the first SVDTFD component. The DWT and the EEMD need to threshold its components, which introduces an extra parameter.

The results obtained in the estimation of the heart rate during physical exercise, allows to conclude that the SVDTFD method outperformed the DWT and EEMD methods.

VI. FUTURE WORK

Future work includes: i) To analyze if the SVDTFD is applicable to other signals. ii) To obtain the heart rate variability from patients in continuous movement with SVDTFD. iii) To analyze the performance of SVDTFD in the measurement of the S_pO_2 by individually filtering the red and IR signals when motion artifacts occurs.

ACKNOWLEDGMENT

This work was financed by "Fondo de Sostenibilidad Universidad de Antioquia - Estrategia de sostenibilidad 2014-2015".

REFERENCES

[1] J. Spigulis, "Optical non-invasive monitoring of skin blood pulsations," in *Optical Materials and Applications*, International Society for Optics and Photonics, 2005, p. 59461R.
[2] A. A. Alian and K. H Shelley, "Photoplethysmography," *Best Practice & Research Clinical Anaesthesiology*, vol. 28, no. 4, pp. 395-406, 2014.
[3] J. G. Webster, *Design of Pulse Oximeters*, CRC Press, 2002.
[4] J. E. Sinex, "Pulse oximetry: Principles and limitations," *The American Journal of Emergency Medicine*, vol. 17, no. 1, pp. 59-67, 1999.
[5] J. Allen, "Photoplethysmography and its application in clinical physiological measurement," *Physiological Measurement*, vol. 28, no. 3, 2007.
[6] K. A. Reddy and V. J. Kumar, "Motion artifact reduction in photoplethysmographic signals using singular value decomposition," in *Proc. IEEE Instrumentation and Measurement Technology Conference*, 2007, pp. 1-4.
[7] H. Han and J. Kim, "Artifacts in wearable photoplethysmographs during daily life motions and their reduction with least mean square based active noise cancellation method," *Computers in Biology and Medicine*, vol. 42, no. 4, pp. 387-393, 2012.
[8] M. Raghuram, K. V. Madhav, E. H. Krishna, and K. A. Reddy, "On the performance of wavelets in reducing motion artifacts from photoplethysmographic signals," in *Proc. 4th International Conference on Bioinformatics and Biomedical Engineering*, 2010, pp. 1-4.
[9] P. P. Kanjilal, J. Bhattacharya, and G. Saha, "Robust method for periodicity detection and characterization of irregular cyclical series in terms of embedded periodic components," *Physical Review E*, vol. 59, no. 4, p. 4013, 1999.
[10] F. Hlawatsch and F. Auger, *Time-Frequency Analysis*, John Wiley & Sons, 2013.
[11] P. Faundez and A. Fuentes, *Procesamiento Digital de Señales acústicas Utilizando Wavelets*, Instituto de Matemáticas UACH, 2000.
[12] Y. Kopsinis and S. McLaughlin, "Development of EMD-based denoising methods inspired by wavelet thresholding," *IEEE Transactions on Signal Processing*, vol. 57, no. 4, pp. 1351-1362, 2009.
[13] N. E. Huang, *et al*., "The empirical mode decomposition and the Hilbert spectrum for nonlinear and non-stationary time series analysis," *Proceedings of the Royal Society of London A: Mathematical, Physical and Engineering Sciences*, vol. 454, pp. 903-995, 1998.
[14] T. Schlurmann, "The empirical mode decomposition and the hilbert spectra to analyse embedded characteristic oscillations of extreme waves," in *Proc. Rogue Waves*, 2001, pp. 157-165.
[15] Z. Wu and N. E. Huang, "Ensemble empirical mode decomposition: A noise-assisted data analysis method," *Advances in Adaptive Data Analysis*, vol. 1, no. 1, pp. 1-41, 2009.
[16] M. A. Colominas, G. Schlotthauer, M. E. Torres, and P. Flandrin, "Noise-Assisted EMD methods in action," *Advances in Adaptive Data Analysis*, vol. 4, no. 4, 2012.
[17] X. Sun, P. Yang, Y. Li, Z. Gao, and Y. T. Zhang, "Robust heart beat detection from photoplethysmography interlaced with motion artifacts based on empirical mode decomposition," in *Proc. EMBS International Conference on Biomedical and Health Informatics*, 2012, pp. 775-778.
[18] Z. Zhang, Z. Pi, and B. Liu, "Troika: A general framework for heart rate monitoring using wrist-type photoplethysmographic (ppg) signals during intensive physical exercise," *IEEE Transactions on Biomedical Engineering*, vol. 62, no. 2, 2014.
[19] J. Rafiee, M. A. Rafiee, N. Prause, and M. P. Schoen, "Wavelet basis functions in biomedical signal processing," *Expert Systems with Applications*, vol. 38, no. 5, pp. 6190-6201, 2011.

Juan Rojano was born in Colombia in 1983. He received his bachelor's degree from National University of Colombia in electrical engineering and his M.Sc. degree from University of Antioquia, specializing in signal processing and clustering.
His research interests include biological signal processing and artificial intelligence. Actually his is an adjunct professor in Electronic Engineering Department at the University of Antioquia.

Dr. Claudia Isaza is an Associate Professor in Electronic Engineering Department at the University of Antioquia, Medellín, Colombia. Her research interests include complex systems monitoring using clustering methods and fuzzy logic.
She received her bachelor's degree in electronic engineering from Distrital F.J.C. University (Bogota-Colombia) in 2002, her M.S. degree in electrical engineering (control emphasis) from Andes University (Bogota-Colombia) in 2004, and her Ph.D. degree in Automatic Systems from INSA, Toulouse, France in 2007.